Proceedings of the IASS Annual Symposium 2023
Integration of Design and Fabrication
10 – 14 July 2023, Melbourne, Australia
Y.M. Xie, J. Burry, T.U. Lee and J. Ma (eds.)

Generation of a compression-tension combined funicular polyhedral beam structure

Hua CHAI[*,a], Yao LU[a], Márton HABLICSEK[b], Masoud AKBARZADEH[a,c]

[*,a] Polyhedral Structures Laboratory, Weitzman School of Design, University of Pennsylvania, Philadelphia, USA
Pennovation Center, 3401 Grays Ferry Ave. Philadelphia, PA, 19146
[*] hchai@upenn.edu

[b]Department of Mathematics, Leiden University, Leiden, Netherlands
[c]General Robotic, Automation, Sensing and Perception (GRASP) Lab, School of Engineering and Applied Science, University of Pennsylvania, Philadelphia, USA

Abstract:
This paper presents a robust form-finding method by implementing algebraic polyhedral graphic statics to generate compression-tension combined beam structure. Compared to iterative graphic statics modeling, the advanced algebraic method can define the inputs and constraints of complex geometries rapidly and precisely. The previous development of the undulating beam system relies on manipulating the Geometric Degree of Freedom (GDoF). The transforming process of GDoF is only operated in form diagram, same force diagram is utilized for finalizing the design with the combination of both form modules. Indeed, investigating these steps from the procedural implementation is not an evident process. In contrast, applying the algebraic method will provide a clearer direction for the user to modify the initial design parameter without extra manual adjustment easily. Moreover, different from the existing algebraic method that needs non-intersected planar surfaces as the potential input to construct the cells, the proposed method is to convert intersected geometries to convex polyhedrons that share the same planar surface as the input. The cells will be flipped by changing the force diagram's normal direction. The presented approach allows for a comprehensive understanding of equilibrium and constraint requirements in form and force diagrams.

Keywords: Form-finding, graphic statics, beam design, algebraic 3D graphic statics

1. Introduction

The pursuit of efficient and innovative structural designs has driven the development and exploration of a wide range of form-finding methods. Graphic statics, a well-established technique, has consistently proven invaluable for designers and engineers over a hundred years [1–3], offering a clear understanding of the relationship between form and forces. The visual and intuitive nature of graphic statics has made it particularly effective for analyzing planar systems.

As an extension of the conventional graphic statics method, 3D Graphic Statics (3DGS) explored the possibilities of designing complex spatial structures. The method allows for the simultaneous analysis of multiple forces acting on the structure, making it easier to consider different loading scenarios and optimize the design accordingly [4, 5]. By understanding the force distribution and equilibrium within the structure, designers can optimize the structural members for material efficiency, minimize weight, and maximize structural performance.

The majority of 3DGS implementations depend on procedural techniques [6] or iterative algorithms that use local node operations [7, 8]. Procedural methods can be time-consuming and difficult to generalize across various inputs, while iterative algorithms based on node operations provide a unified solver, controlling edge lengths, vertex locations, and face areas under a single framework. However, these algorithms require an input angle tolerance for terminating iterations, leading to some deviation in the output and longer runtimes for more complex geometries. Furthermore, they cannot construct reciprocal diagrams for non-convex polyhedrons representing combined tension-compression systems, limiting the solution space exploration.

On the other hand, algebraic formulations of reciprocal diagrams offer an alternative perspective for implementing polyhedron-based 3DGS. These formulations provide more robust and faster numerical processes than existing methods, enabling greater flexibility, reduced computation time, and higher accuracy when manipulating reciprocal diagrams.

1.1. Related work

1.1.1. Computational implementations of 3DGS

Integrating computational methods and digital tools has expanded the scope and potential of polyhedral graphic statics, enabling more efficient analysis and optimization of three-dimensional structures. The properties of polyhedral forms can be combined with various fabrication techniques, such as 3D printing and origami, to create spatial frame systems with diverse design features [9–11]. Moreover, polyhedron-based 3D Graphic Statics can produce cellular solids featuring unique micro-architectures. Current studies demonstrate that subdividing force diagrams by subdivision can change these structures into highly efficient, low-density shellular funicular configurations [12]. These studies illustrate the versatility and effectiveness of polyhedral graphic statics in addressing the challenges of contemporary structural design.

1.1.2. Algebraic graphic statics

Alongside the traditional graphical approach in 2D graphic statics, researchers have explored incorporating algebraic methods, which streamline the analysis and design process for two-dimensional structures by formulating and solving equilibrium equations. Micheletti [13] introduced the concept of algebraic duality in reciprocal diagrams of self-stressed frameworks, which was then termed algebraic graphic statics by Van Mele and Block [14]. This tool calculates internal force distribution using connected lines as input and derives edge lengths by ensuring the 2D closeness of polygons. This method allows for obtaining internal and external force magnitudes. Alic and Åkesson [15] later extended this to a bi-directional approach, enabling manipulation of both force and form diagrams and updating reciprocal diagrams instantly, making it an effective interactive form-finding tool in 2D.

1.1.3. Algebraic 3D graphic statics

Building upon the principles of graphic statics, the methodology has been developed to incorporate three-dimensional systems, leading to the establishment of algebraic 3D graphic statics. Hablicsek et al. [16] developed an algebraic framework for 3D Graphic Statics, where reciprocal polyhedral diagrams are represented by a linear system of equations ensuring planar closeness of polyhedron faces. This method computes dual diagrams with high accuracy and allows for user input to control edge lengths, offering flexibility in exploring the solution space [17]. However, it lacks precise control over vertex location and edge lengths. Akbarzadeh and Hablicsek [18] proposed a quadratic formulation that can handle assigned area and edge lengths, enabling manipulation of force diagrams with desired face areas and exploration of various equilibrium states.

1.2. Problem statement and objectives

As previously discussed, 3DGS has demonstrated significant potential for diverse applications across various materialization strategies. However, current implementations have yet to take full advantage of the capabilities that 3DGS has to offer. For instance, the iterative method is limited to compressive

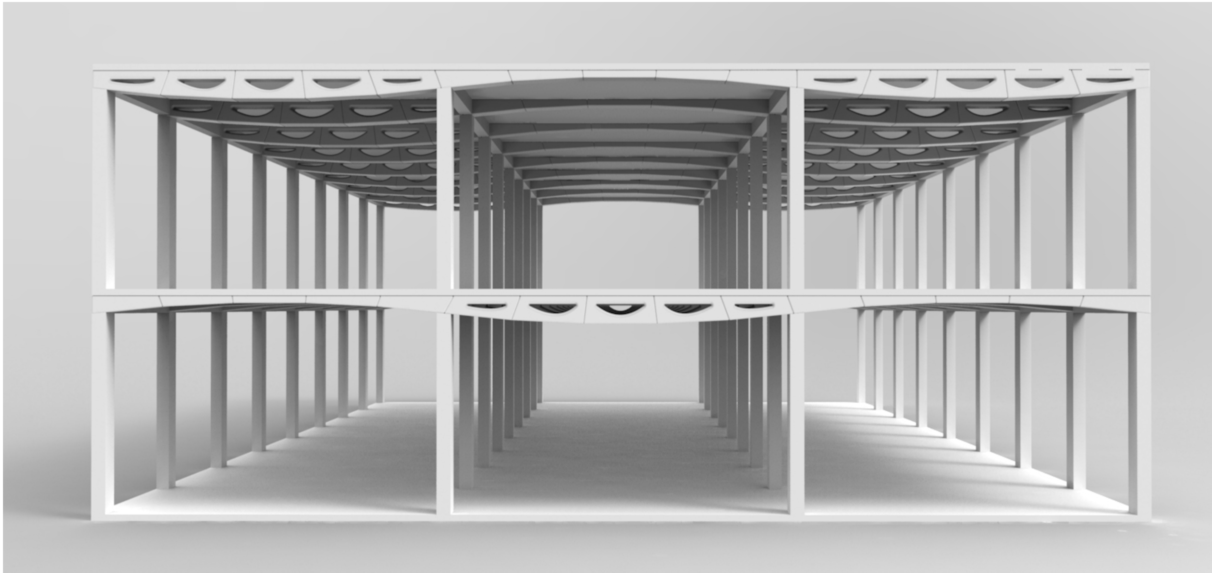

Figure 1. Undulating beam structure with potential porous materialization for all the modules.

form finding, which is usually utilized for the compression-dominant structure and is computationally demanding for intricate geometries.

While the algebraic formulation of 3DGS allows for a comprehensive exploration of the solution space, it needs to have the same precision in controlling edge lengths in reciprocal diagrams that the iterative method provides. This is a crucial aspect that needs to be addressed to maximize the potential of 3DGS for practical applications.

The other challenging part of the method is to develop an efficient and robust way for form-finding to further determine an updated force diagram and generate a corresponding form diagram that satisfies these constraints. This process should apply to a wide range of complex three-dimensional structures, facilitating the analysis and optimization of form and forces in spatial systems. To address the problem stated above, the following objectives have been identified:

- Check the property of the geometric relationships that define the force groups, including global, compression, and tension.

- Develop an algorithm that uses algebraic edge constraints to update the force diagram and generate a corresponding form diagram that adheres to these constraints.

- Demonstrate the effectiveness and versatility of the proposed method through the case study of an undulating beam structure that represents the compression and tension combined loading scenarios.

To tackle these issues, this paper aims to present an enhanced algebraic formulation of 3DGS that incorporates edge constraints. This advanced formulation offers precise control over edge lengths without compromising the inherent advantages of flexibility and accuracy. A more detailed explanation of vertex constraint can be found in the research of Lu et al. [19].

2. Methodology

In this section, we present the methodology of algebraic 3DGS, specifically focusing on the utilization of edge constraints to design structures that incorporate both compression and tension nodal groups. As the continuation study of the previous research [20], we will demonstrate the design process through the example of the same repeatable undulating beam structure shown in Figure 1.

In 3DGS, polyhedral reciprocal diagrams play a crucial role in representing both form and force diagrams. These diagrams feature a well-defined topological and geometrical hierarchy, including vertices (v), edges (e), faces (f), and cells (c). The unique arrangement within these diagrams ensures that each edge shares a common vertex with its adjacent edges. The edges and faces in reciprocal diagrams exhibit specific directions, which are essential for maintaining the structural integrity of the diagrams. The right-hand rule is applied to achieve consistency, guiding the alignment of face normals and edge directions [16]. This rule ensures that face orientations remain consistent within each cell and maintain cell orientations throughout the diagram. As a result of this structure, neighboring faces in the reciprocal diagrams share two versions of the same edge but with opposing directions. Similarly, adjacent cells exhibit two versions of an identical face, each with contrasting normal directions. This detailed arrangement showcases the intricacies of the polyhedral reciprocal diagrams in 3DGS and their significance in both form and force representation.

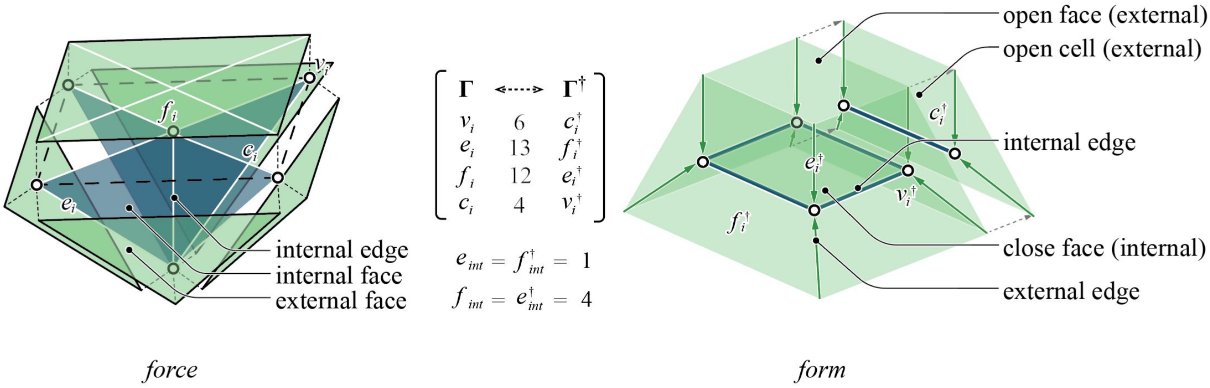

Figure 2. Left: force diagram; Right: form diagram.

A four-applied loads example is illustrated to show the topological relationship between polyhedral diagrams (Figure 2). The starting diagram or the first input is called *primal*, Γ, which can either be a form diagram or a force diagram and the reciprocal diagram is called *dual*, $\Gamma^\dagger$. The ones of the dual are identified as a dagger symbol (†). In general, both two diagrams share a reciprocal relationship, with the primal diagram's elements—vertices v, edges e, faces f, and cells c—mapping to the corresponding elements in the dual diagram—cells ($c^\dagger$), faces ($f^\dagger$), edges ($e^\dagger$), and vertices ($v^\dagger$). This reciprocity leads to an equal number of dual elements in both diagrams, such as the primal's edges (e) matching the dual's faces ($f^\dagger$) and the primal's vertices (v) matching the dual's cells ($c^\dagger$). Additionally, adjacency is preserved between the corresponding elements in both diagrams and each edge (e_i) in the primal is perpendicular to its corresponding face ($f_i^\dagger$) in the dual.

The force diagram's external faces correspond to the external edges in the form diagram that represent applied loads and reaction forces, typically depicted in green. While all elements in the force diagram are closed, the form diagram contains open elements. External edges in the form diagram have vertices at only one end, making them open-ended, and any faces or cells with open edges are also considered open. In contrast, closed faces in the form diagram are deemed internal and correspond to the force diagram's internal edges.

2.1. Analysis of form and force diagrams

The previous IASS paper presented an initial form generated using 2D graphic statics, which was then manipulated geometrically to increase design freedom for constructing updated modules. Detailed force distribution was also utilized to locate the column when merging the two units together. Figure 3 shows the extruded version of single force diagram connecting two modules that are generated from GDoF. The applied loads are evenly distributed at the top, and the supports are illustrated to identify the merging locations.

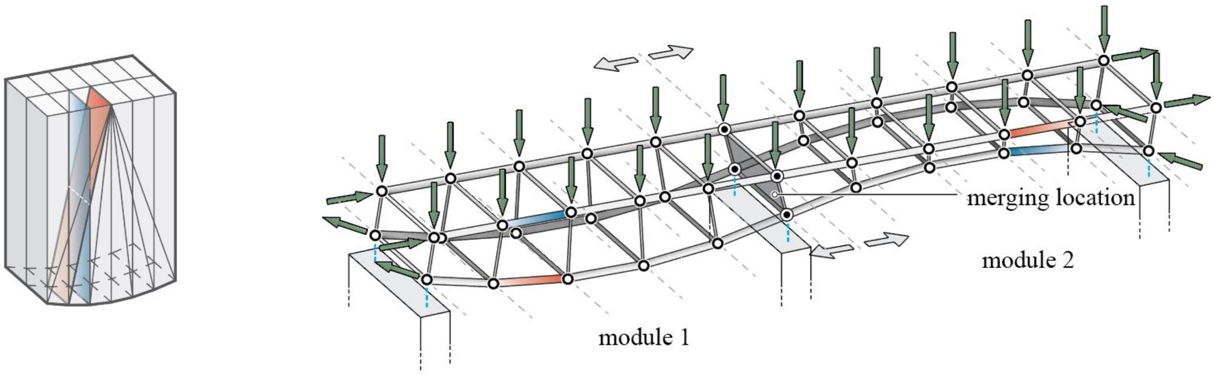

Figure 3. Left: single force diagram of two modules combined; Right: its corresponding form diagram shows the undulation of the geometry and the merging location.

Considering the current limitations of the algebraic graphic statics method, which does not allow intersected faces as input parameters, it is essential to analyze the geometric relationship of the initial force diagram. This analysis enables designers to gain a deeper understanding of structural behavior, paving the way for the development of improved methods and approaches that address these limitations. The key idea focuses on transforming intersected cells into non-intersected convex cells. Investigating this transformation process can help uncover potential strategies to overcome the existing constraints. Importantly, the geometric data is contained within the individual elements. The original relationship is preserved as long as the geometry remains unaltered by adding or subtracting faces, allowing for the free manipulation of moving locations. This approach offers a promising avenue for enhancing the applicability and effectiveness in solving complex geometric problems.

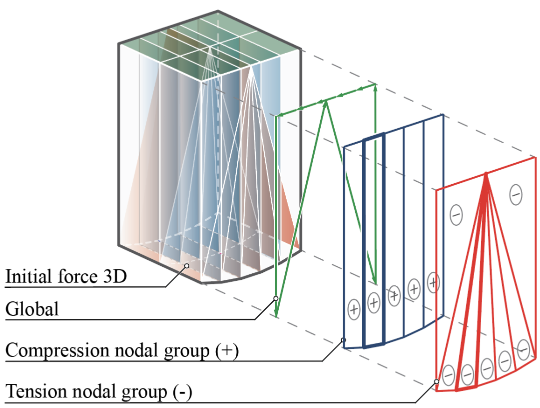

Figure 4. Analysis of different nodal groups in the tension and compression combined force diagram.

Figure 4 presents a detailed representation of the various nodal groups within the force diagram, effectively dividing it into global, compression, and tension forces. To classify these groups based on the connection to the global forces, a positive (+) value represents the compression that shared the edges with applied loads, and the negative (-) is for tension cells that have the same edges with reaction forces. The force diagram effectively demonstrates the intricate relationships in 2D, describing the connections between the edges. In the case of the 3D version, it is essentially a simple extrusion from the 2D representation, maintaining the same relationships between the elements. The global forces, denoted by the color green, remain unchanged throughout the process.

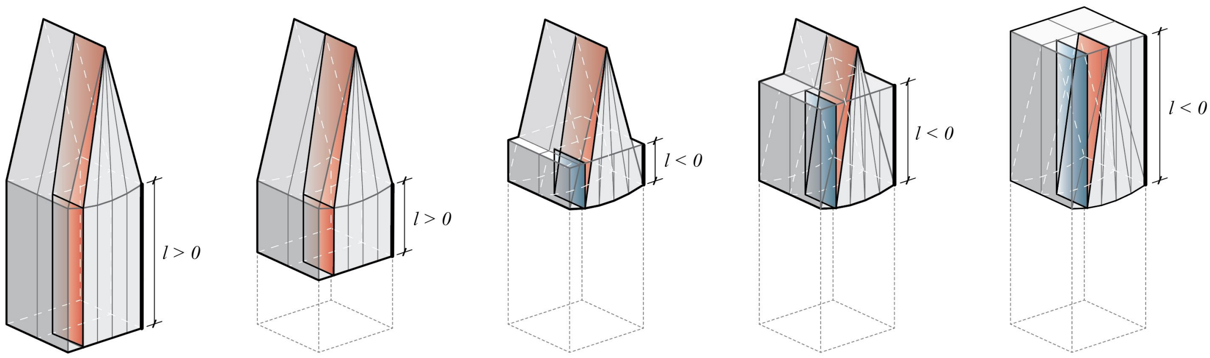

Figure 5. Edge length switched from a positive number to negative to finalize the form diagram.

2.2. Algebraic form-finding

In this section, the equilibrium equation of algebraic implementation will be explained. Firstly, each edge of the force diagram is perpendicular to its corresponding face in the form diagram, resulting in the unit direction vector of edge $e_i^\dagger$ in the form diagram being equal to the unit normal vector of face f_i in the force diagram. Then define $\mathbf{N}x$, $\mathbf{N}y$, and $\mathbf{N}z$ as $[f_{int} \times f_{int}]$ diagonal matrices with diagonal entries representing the x-, y-, and z- coordinates of the unit normal vectors of the internal faces in the force diagram, respectively. Based on prior research in the algebraic method, the $[e_{int} \times f_{int}]$ connectivity matrix $\mathbf{C}_{e_{int} \times f_{int}}$ displays the relationship between faces and edges in the form diagram. Consequently, the closeness can be expressed accordingly:

$$\begin{aligned} \mathbf{C}_{e_{int} \times f_{int}} \mathbf{N}_x \mathbf{q} = \mathbf{0} \\ \mathbf{C}_{e_{int} \times f_{int}} \mathbf{N}_y \mathbf{q} = \mathbf{0} \\ \mathbf{C}_{e_{int} \times f_{int}} \mathbf{N}_z \mathbf{q} = \mathbf{0} \end{aligned} \tag{1}$$

Combing the above equations to an equilibrium matrix multiple by the potential edge length as shown here:

$$\mathbf{A}\mathbf{q} = \mathbf{0} \tag{2}$$

so $\mathbf{A}$ is a $[3e_{int} \times f_{int}]$ equilibrium matrix can be represented as

$$\mathbf{A} = \begin{pmatrix} \mathbf{C}_{e_{int} \times f_{int}} \mathbf{N}_x \\ \hline \mathbf{C}_{e_{int} \times f_{int}} \mathbf{N}_y \\ \hline \mathbf{C}_{e_{int} \times f_{int}} \mathbf{N}_z \end{pmatrix} \tag{3}$$

Every solution for $\mathbf{q}$ represents a potential combination of edge lengths in the form diagram that ensures the closeness of all internal faces within the form diagram.

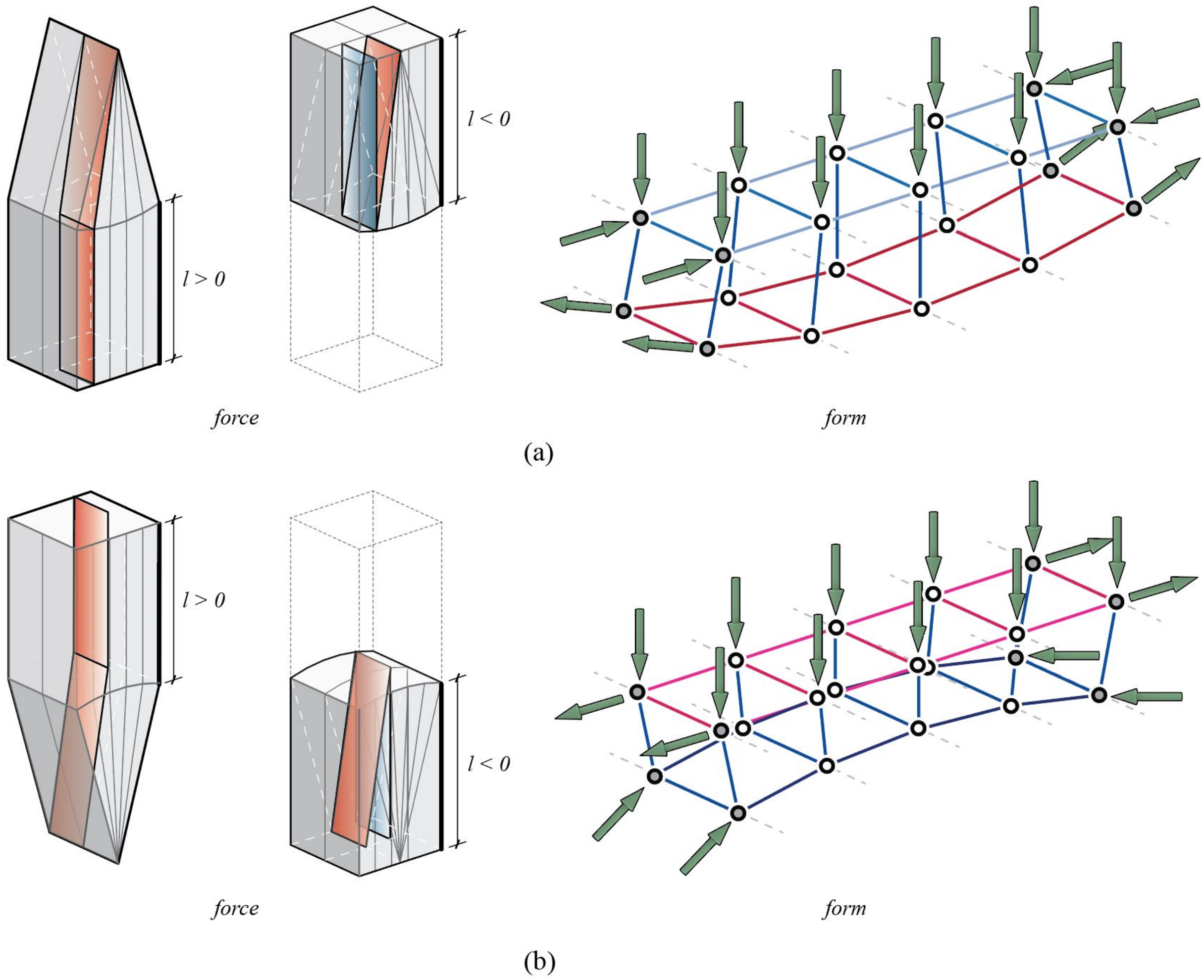

Figure 6. The transition from compression/tension only to intersected force diagram and corresponding form diagram. (a) the reciprocal polyhedral diagrams of the first module (b) mirrored force diagram as the input to generate the second module.

2.3. Additional edge constraints operation

Edge constraints set target lengths for the internal edges in the form diagram, and each constrained edge requires one additional constraint equation. For example, if the i-th internal edge $e_i^\dagger$ is constrained to a target length l, its constraint equation may be written as

$$\mathbf{b}_i^\intercal \mathbf{q} = l \tag{4}$$

where $\mathbf{b}_i$ is the $[f_{int} \times 1]$ column vector with all entries zero (0) except at the index of $e_i^\dagger$ where it's one (1). For a total number of b constrained edges, all b edge constraint equations may be assembled in the matrix form as

$$\mathbf{Bq} = \mathbf{l} \tag{5}$$

where the rows of the $[b \times f_{int}]$ edge constraint matrix $\mathbf{B}$ are the row vectors $\mathbf{b}_i^\intercal$, and $\mathbf{l}$ is a $[b \times 1]$ column vector with the entries being the target lengths.

2.4. Constrained solutions

All equilibrium equations, edge constraint equations, and vertex constraint equations are assembled as a system of non-homogeneous constrained linear equilibrium equations written as follows:

$$\mathbf{Mq} = \mathbf{t}. \tag{6}$$

Here the $[(2e_{int} + b + 3(p-1) + 2l + n) \times f_{int}]$ matrix $\mathbf{M}$ is named the constrained equilibrium matrix, obtained by vertically stacking the equilibrium matrix $\mathbf{A}$ and the edge constraint matrix $\mathbf{B}$

$$\mathbf{M} = \begin{pmatrix} \mathbf{A} \\ \mathbf{B} \end{pmatrix}. \tag{7}$$

The $[(2e_{int} + b + 3(p-1) + 2l + n) \times 1]$ column vector $\mathbf{t}$ is obtained by vertically stacking the $[2e_{int} \times 1]$ zero vector, the vector $\mathbf{l}$, and the vector $\mathbf{d}$. Each solution of $\mathbf{q}$ represents a set of edge lengths of the form diagram that satisfy all equilibrium requirements and constraints.

The form diagram may face issues of over-constraining when constraints conflict with planarity or compete with each other, leading to overdetermined equilibrium equations with no solution. In these cases, the least-square solution offers the closest possible solution by minimizing the Euclidean norm while still attempting to satisfy all equilibrium and constraint requirements.

Figure 5 describes a process by which the final force diagram for the structure can be generated. This is achieved by assigning negative values to specific edges, allowing the structure's bottom part to merge with the top part. The decision to assign negative values is based on the changeable edge length, which affects the force distribution in the structure. It is important to note that the IDs of the fixed edges must be determined to ensure that the structure shifts within the predefined boundary conditions. This is necessary to prevent the structure from moving beyond acceptable limits.

3. Conclusion and future work

In conclusion, this research presents an analysis of the topological relationship between reciprocal polyhedral diagrams. The connectivity matrix and equilibrium matrix are used to express the closeness between the force diagram and its corresponding form diagram. Additional linear equations are introduced to account for edge constraints, resulting in a system of non-homogeneous constrained linear equilibrium equations. The least-square solution is utilized to find the closest solution in cases of over-constraining or incompatibilities among constraints (Figure 6). This approach enables a comprehensive understanding of the equilibrium and constraint requirements in form and force diagrams, paving the way for further exploration and optimization in structural design.

Acknowledgements

This research is funded by the Advanced Research Projects Agency–Energy (ARPA-E) of the U.S. Department of Energy (DE-AR0001631) and the National Science Foundation CAREER Award (NSF CAREER-1944691 CMMI) and the National Science Foundation Future Eco Manufacturing Research Grant (NSF, FMRG-2037097 CMMI) to Dr. Masoud Akbarzadeh.

References

[1] K. Culmann, *Die Graphische Statik*. Zürich: Verlag Meyer und Zeller, 1864.

[2] L. Cremona, *Graphical Statics: Two Treatises on the Graphical Calculus and Reciprocal Figures in Graphical Statics. Translated by Thomas Hudson Beare*. Oxford: Clarendon Press, 1890.

[3] J. C. Maxwell, "On Reciprocal Figures and Diagrams of Forces," *Philosophical Magazine Series 4*, vol. 27, no. 182, pp. 250–261, 1864.

[4] M. Akbarzadeh, T. Van Mele, and P. Block, "3D Graphic Statics: Geometric Construction of Global Equilibrium," in *Proceedings of the International Association for Shell and Spatial Structures (IASS) Symposium*, 2015.

[5] A. McRobie, W. Baker, T. Mitchell, and M. Konstantatou, "Mechanisms and States of Self-stress of Planar Trusses Using Graphic Statics, part II: Applications and Extensions," *International Journal of Space Structures*, vol. 31, no. 2-4, pp. 102–111, 2016. [Online]. Available: http://dx.doi.org/10.1177/0266351116660791

[6] M. Akbarzadeh, "3d graphic statics using reciprocal polyhedral diagrams," Ph.D. dissertation, ETH Zurich, Zurich, Switzerland, 2016.

[7] PSL, "PolyFrame," https://www.food4rhino.com/app/polyframe, Aug 2018. [Online]. Available: https://www.food4rhino.com/app/polyframe

[8] A. Nejur and M. Akbarzadeh, "Polyframe, efficient computation for 3d graphic statics," *Computer-Aided Design*, vol. 134, p. 103003, May 2021.

[9] M. Akbarzadeh, A. Tabatabaie Ghomi, M. Bolhassani, M. Akbari, A. Seyedahmadian, J. Sun, H. Yao, , J. Miziumski, and K. Papalexiou, "Saltatur: Node-based assembly of funicular spatial concrete," in *Proceedings of the 40th Annual Conference of the Association for Computer-Aided Design in Architecture (ACADIA)*, 2021.

[10] Y. Lu, M. Cregan, P. Chhadeh, A. Seyedahmadian, M. Bolhassani, J. Schneider, J. Yost, and M. Akbarzadeh, "All glass, compression-dominant polyhedral bridge prototype: form-finding and fabrication," in *Proceedings of IASS Symposium and Spatial Structures Conference 2020/21, Inspiring the next generation*, Guildford, UK, August 23-27 2021.

[11] M. Akbari, Y. Lu, and M. Akbarzadeh, "From design to the fabrication of shellular funicular structures," in *Proceedings of the Association for Computer-Aided Design in Architecture (ACADIA)*, 2021.

[12] M. Akbari, A. Mirabolghasemi, M. Bolhassani, A. Akbarzadeh, and M. Akbarzadeh, "Strut-based cellular to shellular funicular materials," *Advanced Functional Materials*, p. 2109725, 2022.

[13] A. Micheletti, "On generalized reciprocal diagrams for self-stressed frameworks," *International Journal of Space Structures*, vol. 23, no. 3, p. 153–166, Sep 2008.

[14] T. Van Mele and P. Block, "Algebraic graph statics," *Computer-Aided Design*, vol. 53, pp. 104 – 116, 2014. [Online]. Available: http://www.sciencedirect.com/science/article/pii/S0010448514000682

[15] V. Alic and D. Åkesson, "Bi-directional algebraic graphic statics," *Computer-Aided Design*, vol. 93, pp. 26 – 37, 2017. [Online]. Available: http://www.sciencedirect.com/science/article/pii/S0010448517301446

[16] M. Hablicsek, M. Akbarzadeh, and Y. Guo, "Algebraic 3d graphic statics: Reciprocal constructions," *Computer-Aided Design*, vol. 108, pp. 30 – 41, 2019. [Online]. Available: http://www.sciencedirect.com/science/article/pii/S0010448518303026

[17] M. Akbarzadeh and M. Hablicsek, "Algebraic 3d graphic statics: Constrained areas," *arXiv preprint arXiv:2007.15133*, 2020.

[18] M. Akbarzadeh and M. Hablicsek, "Algebraic 3d graphic statics: Constrained areas," *Computer-Aided Design*, vol. 141, p. 103068, Dec 2021.

[19] Y. Lu, M. Hablicsek, and M. Akbarzadeh, "Algebraic 3d graphic statics with edge and vertex constraints: A comprehensive approach to extending the solution space for polyhedral form-finding," *Computer-Aided Design*, In peer-review.

[20] H. Chai, M. Bolhassani, and M. Akbarzadeh, "Structural form-finding of multi-span undulating funicular beam structure," in *Proceedings of IASS 2022 symposium affiliated with APCS 2022 conference*, Beijing, China, September 19-22 2022.